Journal of Thermal Analysis and Calorimetry (2019) 136:601–608
https://doi.org/10.1007/s10973-018-7669-x

Study of nanocarbon black as synergist on improving flame retardancy of ethylene-vinyl acetate/brucite composites

Zhiqi Liu[1,2] · Yanling Zhang[1,3] · Na Li[1,2] · Xin Wen[4] · Luis Arevalo Nogales[5] · Lijuan Li[1,2] · Fan Guo[1,2]

Received: 18 April 2018 / Accepted: 15 August 2018 / Published online: 24 August 2018

Abstract
Nanocarbon black (CB) was introduced into ethylene-vinyl acetate/brucite (EM) composites to investigate the synergistic effect of CB and metal hydroxide on improving the flame retardancy of EVA. Flammability properties of the as-prepared EVA composites were investigated by thermogravimetric analysis, limiting oxygen index (LOI), UL-94 test and cone calorimetry test. The results indicated that the optimum mass ratio of CB/brucite was 1/54, at which the EVA composites displayed dramatic improvement on thermal stability and flame retardancy. The LOI value was as high as 35.3%, the UL-94 passed the V-0 rating, and the peak heat release rate reduced 79% in comparison with pure EVA. Based on the morphology and structure analysis for residue chars, the flame-retardant mechanism was attributed mainly to the positive synergistic effect of CB and brucite on promoting the formation of better carbon protective layer during combustion.

Keywords Ethylene-vinyl acetate · Brucite · Carbon black · Flame retardant · Synergy

Introduction

EVA, as a typical copolymer, is widely used in numerous applications, such as electronic devices, buildings, packaging, biomedical materials or children toys, due to its good mechanical and physical properties [1]. However, EVA has a high flammability, which makes it burn at a high speed and generate a large amount of heat, and it seriously restricts the applications of EVA in many fields with high demand on flame retardancy [2, 3]. In order to overcome this drawback, one of the most effective ways is to add various flame retardants [4]. It is widely known that halogen-containing flame retardants have high flame-retardant efficiency, but they produce large quantities of smoke, corrosive and toxic gases while burning [5–7]. Therefore, the exploration of nontoxic and environmental-friendly flame retardants for EVA has been an urgent task.

In recent years, people are paying advanced attention to develop halogen-free flame retardants for polymers. As a metal hydroxide filler, magnesium hydroxide (MH) was widely used to prepare flame-retardant composites [8, 9]. There were many reports about its application in polymers, such as EVA [10, 11], poly(vinyl chloride) [12], polypropylene [13, 14], polyethylene [15], polyethylene terephthalate [16] or epoxy resin [17], due to its abundant resources, low cost, high thermal stability and good smoke suppression. However, to achieve a desired flame retardancy effect, generally a great amount of fillers are required in the polymer composites (more than 50%), which results in the deterioration of the mechanical properties of polymers [17–20]. To reduce the negative effects of MH in polymer systems, an effective way is to

✉ Zhiqi Liu
zqliu@isl.ac.cn

[1] Key Laboratory of Comprehensive and Highly Efficient Utilization of Salt Lake Resources, Qinghai Institute of Salt Lakes, Chinese Academy of Sciences, Xining 810008, China

[2] Qinghai Engineering and Technology Research Center of Comprehensive Utilization of Salt Lake Resources, Xining 810008, China

[3] Key Laboratory of Salt Lake Geology and Environment of Qinghai Province, Xining 810008, China

[4] Nanomaterials Physicochemistry Department, Faculty of Chemical Technology and Engineering, West Pomeranian University of Technology in Szczecin, al. Piastów 45, 70-311 Szczecin, Poland

[5] Universidad Politécnica de Madrid, E.T.S. de Ingenieros de Caminos, 28040 Madrid, Spain

incorporate other nanofillers to achieve synergetic enhancement in the principle of making best use of advantages and bypassing the disadvantages. In recent years, many researchers have published the synergism of flame retardancy, such as silica [10, 21], zinc borate [11], multiwall carbon nanotube [19], nanoclay [22], hollow glass [23]and expandable graphite [24], combined with MH.

Nanosized carbon materials have attracted a great deal of attention in the past few decades because of their advantageous characteristics [25–27], such as low density, high thermal stability and good conductivity. [28, 29]. The previous reports have revealed that nanocarbon black could increase thermal stability and flame retardancy of polyolefin due to its trapping radical effect during the burning of composites [30–32]. In comparison with micron-sized additives, nanomaterials showed several advantages, especially with respect to significantly reducing the heat release rate at quite low loading (less than 5%) [29, 31, 33, 34]. To the best of our knowledge, there are no reports about synergistic flame-retardant effects of CB in EVA/brucite system.

In this work, EVA/brucite/CB (EMC) were prepared to investigate the positive effects of CB in an EM flame-retardant system. Their flame retardancy and thermal stability were investigated by LOI, UL-94 test, CCT and TG. Furthermore, their mechanical properties were evaluated by tensile test.

Experimental

Materials

Ethylene-vinyl acetate (EVA) copolymer (Elvax-265, containing 28% vinyl acetates with a melt flow rate of 3 g 10^{-1} min^{-1}) was supplied by DuPont Company (USA). Brucite (mineral form of MH, with the content of magnesium oxide more than 69%) was kindly supplied by Liaoning Kuandian (Liaoning, China). Carbon black (CB, purity: > 99%) was purchased from Linzi Qishun Chemical Co., Shandong, with the original particle diameter of 17 nm. All the samples were dried in a vacuum oven at 80 °C for 12 h before processing.

Preparation of the flame-retardant EVA composites

All the samples were prepared with the same procedure by melt intercalation method using a microcompounder (MC-15, Xplore Instruments BV, Newsland). The processing of the composites was carried out at a temperature of 180 °C with a screw speed of 50 rpm and residence time of 15 min. For the properties tests, different standard testing bars, according to the standards mentioned in the following part, were obtained by using a hot press machine. All the samples were dried in a vacuum oven at 80 °C for 2 h before processing. The formulations are given in Table 1.

Characterization

Thermogravimetric analysis (TG) was determined from room temperature to 600 °C, with a heating rate of 10 °C min^{-1} in nitrogen atmosphere with a flow speed of 90 mL min^{-1}, using a TA thermogravimetric analyzer (Q50, USA). All the samples were dried in a vacuum oven at 80 °C for 2 h before test.

Limiting oxygen index (LOI) was measured by oxygen index meter (FTT, UK) with sheet dimension of 130 × 6.5 × 3.2 mm^3, according to ASTM D 2863-77 standard.

Vertical burning test was carried out on UL-94 vertical flame chamber (FTT, UK) with dimensions of 130 × 13 × 3.2 mm^3, according to ASTM D3801 standard.

The fire behavior of the samples was performed on cone calorimeter (FTT, UK), according to the ISO 5660 standard, under a heat flux of 50 kW m^{-2} with a sample size of 100 × 100 × 3 mm^3.

Tensile testing was performed on a universal electromechanical testing machine (INSTRON 3384, USA) according to ASTM D 638 standard at a test speed of 50 mm min^{-1}.

A Zeiss, EVO MA15 (Germany) scanning electron microscope equipped with energy dispersive spectra (EDS) was utilized to characterize the microstructure of the char layer after cone calorimeter test.

Results and discussion

Thermal stability of EVA composites

The thermal stability of EVA and its composites with a different content of CB was investigated by TG in nitrogen

Table 1 Formulations of the EVA composites

Sample code	EVA/%	Brucite/%	CB/%
EVA	100.0	0.0	0.0
EM	45.0	55.0	0.0
EMC 1	45.0	54.5	0.5
EMC2	45.0	54.0	1.0
EMC3	45.0	53.0	2.0
EMC4	45.0	52.0	3.0

atmosphere. Figure 1 shows the TG and the derivative thermogravimetric (DTG) curves, and the corresponding data are listed in Table 2. The temperatures at which 10% ($T_{-10\%}$), 50% ($T_{-50\%}$) and maximum (T_{max}) mass loss occurs were used as the measure of the initial degradation temperature, half degradation temperature and maximum degradation temperature, respectively. It was observed that the thermal degradation of pure EVA and its composites was a two-step degradation—elimination of the side group with acetic acid release and then breaking of the main chain [5, 23]. The $T_{-10\%}$, $T_{-50\%}$, T_{max1} and T_{max2} for pure EVA were 320 °C, 426 °C, 325 °C and 439 °C, respectively. Compared with pure EVA, the $T_{-10\%}$, $T_{-50\%}$, T_{max1} and T_{max2} values of EM increased to 334 °C, 461 °C, 338 °C and 459 °C, respectively. However, the $T_{-10\%}$, $T_{50\ \%}$, T_{max1} and T_{max2} values of EVA composites with brucite and CB were highest and increased to 352 °C, 485 °C, 356°C and 480 °C, respectively. The results showed that the use of brucite and CB upgraded the thermal stability of the composites, and CB had an obvious synergistic effect on the system. However, the amount of residues of EMC did not show distinct change, indicating that the presence of CB in EMC did not induce catalytic carbonization effect.

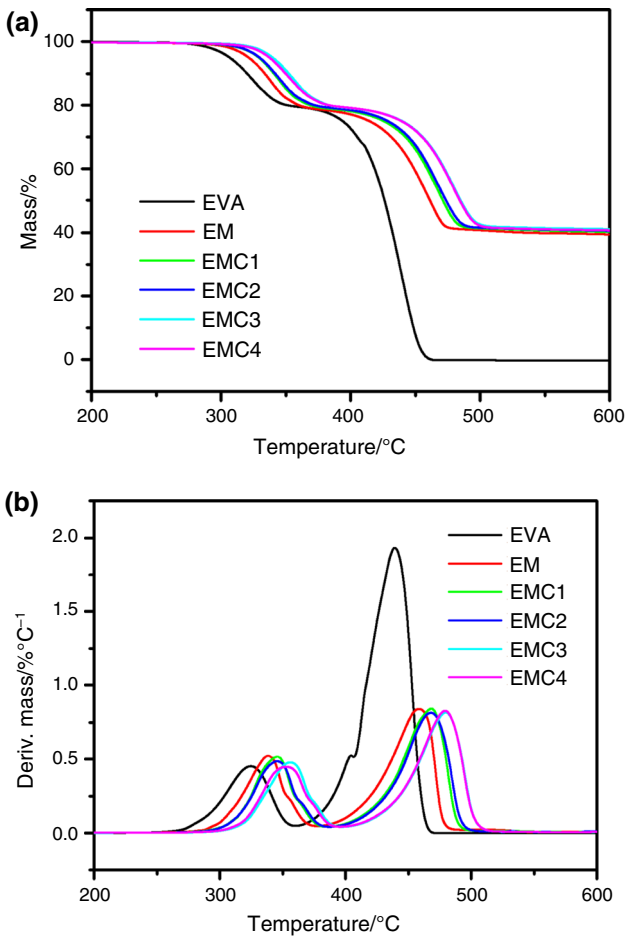

Fig. 1 TG (**a**) and DTG (**b**) curves of pure EVA and its composites at a heating rate of 10 °C min^{-1} in nitrogen

Table 2 TG and DTG data of pure EVA and its composites in nitrogen

Samples	$T^{a}_{-10\%}$/°C	$T^{b}_{-50\%}$/°C	T^{c}_{max1}/°C	T^{d}_{max2}/°C	Mass[e]/%
EVA	320	426	325	439	0
EM	334	461	338	459	39.4
EMC1	341	471	345	468	40.2
EMC2	342	474	346	468	40.6
EMC3	352	485	356	480	41.1
EMC4	349	484	353	479	41.7

[a]Temperature at 10% mass loss

[b]Temperature at 50% mass loss

[c]Temperature at the first maximum mass loss rate

[d]Temperature at the second maximum mass loss rate

[e]Residue at 600 °C

LOI and UL-94

In this segment, the effect of brucite and different contents of CB on the flammability of EVA was investigated by limiting oxygen index (LOI) and vertical burning test (UL-94). Table 3 shows the results for pure EVA and its composites. It could be seen from Table 3 that the LOI value of pure EVA was only 18.5%. When brucite was added, the LOI value of EM increased to 34.0%. As for EMC, with the increase in CB content from 0.5 to 1.0%, the LOI value gradually increased. However, with further increase of CB content more than 1.0%, the LOI exhibited a small decrease, which suggested that 1% was a proper content of CB with best flame retardancy in our EVA system. The UL-94 results showed that the pure EVA had no-rating, while the EM could reach V-1; especially, the dripping of pure EVA also was serious. After the combination of CB

Table 3 Results obtained from LOI and UL-94 tests

Samples	LOI/%	UL-94 (thickness at 3.2 mm)			
		t_1/s	t_2/s	Rating	Dripping
EVA	18.5	/	/	Fail	Yes
EM	34.0	3	9	V-1	No
EMC1	34.8	2	1	V-0	No
EMC2	35.3	1	1	V-0	No
EMC3	34.6	1	1	V-0	No
EMC4	34.3	1	1	V-0	No

and brucite, all composites passed the V-0 rating and demonstrated higher flame retardancy. Obviously, all the additions of brucite and CB reduced the flammability of EVA. For the EMC2 sample with 54% brucite and 1% CB, the LOI reached the maximum value of 35.3%, which means that EMC2 has the best flame retardancy in EVA matrix. Table 4 also shows that all the flame-retardant EMC samples reached V-0 level. On the basis of the above results, CB was an effective synergist in EM system.

Combustion behavior

To further investigate the effect of CB in EM composites, the combustion behavior of EVA and its composites was investigated by cone calorimetry test, and the related data are summarized in Table 5. The heat release rate (HRR), total heat release (THR), smoke release rate (SRR) and total smoke release (TSR) curves versus the burning time for EVA and its composites are presented in Figs. 2, 3, 4 and 5, respectively.

From Fig. 2, it could be found that the pure EVA was easily flammable after ignition and exhibited a sharp HRR curve at 125 s, and the peak value of HRR was as high as 1139 kWm^{-2}. When 55% of brucite was added to EVA, the EM sample burned slowly compared with pure EVA and the PHRR decreased to 357 kWm^{-2}. Furthermore, after the CB was added into the EM systems, the EMC samples burned more slowly than pure EVA and EM. The HRR curve of EMC2 with the content of 1% CB is shown to be smoothest and lowest of the curves. At the end of burning, as shown in Fig. 3, pure EVA released a total heat of 110 kJ m^{-2}. The THR values for EMC2 were decreased to 75 kJ m^{-2}, and the reduction in THR was around 32%. The reduction in HRR and THR of EMC composites indicated that the CB participated in the carbonization process and was kept in the condensed phase, which was in accordance with the TG and residual char results. Lower HRR and THR values were crucial for saving lives and assets during a fire.

Smoke production during combustion is another very important factor in fire safety fields [35, 36]. It is reported that the acute toxicity of fire gases is mainly responsible for over 70% of people killed by fires. From Fig. 4, the SPR curve of pure EVA was the highest and sharpest one among the samples, and its peak value was 0.084 $m^2\ s^{-1}$. The peak in the SPR curve of EM was 0.040 $m^2\ s^{-1}$. The SPR curve of EMC2 was lowest and smoothest among all the samples, with a peak value of 0.021 $m^2\ s^{-1}$. Compared with pure EVA, the reduction of the peak values in the SPR curve was 52.38% and 65.48%. Figure 5 presents the total smoke production of pure EVA and flame-retardant EVA composites. The TSR of pure EVA was 10.03 $m^2\ m^{-2}$, and the TSR of EM was 5.97 $m^2\ m^{-2}$. Additionally, meanwhile, it was observed that the TSR values decreased greatly with the addition of CB in the EVA and brucite system, being the EMC2, with the 1% of CB, the lowest among all the samples. It demonstrated that an appropriate amount of CB

Table 5 Mechanical properties of pure EVA and its composites

Samples	Tensile stress/MPa	Elongation at break/%
EVA	22.7	1297
EM	11.1	104
EMC1	11.4	109
EMC2	11.4	106
EMC3	11.4	101
EMC4	11.2	100

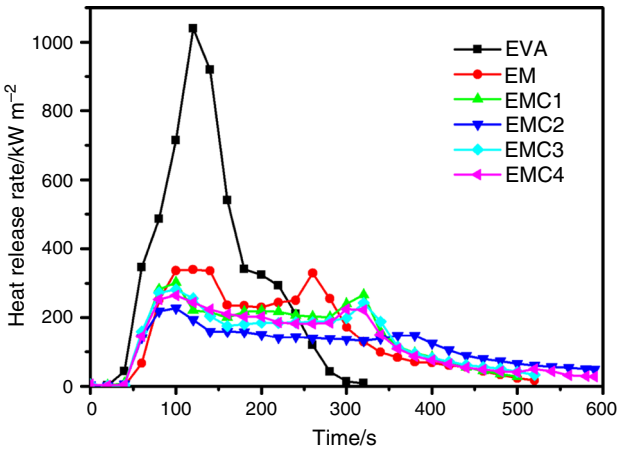

Fig. 2 Heat release rate curves of EVA and its composites from cone calorimeter test

Table 4 Combustion parameters obtained from cone calorimeter test

Samples	t_{ign}/s	PHRR/kW m^{-2}	THR/MJ m^{-2}	SPR/$m^2\ s^{-1}$	TSR/$m^2\ m^{-2}$	Residue/%
EVA	36 ± 2	1139 ± 15	110 ± 10	0.084	10.03	0.0
EM	55 ± 2	357 ± 10	79 ± 5	0.040	5.97	40.4
EMC1	44 ± 2	302 ± 10	77 ± 5	0.029	5.33	41.6
EMC2	42 ± 2	238 ± 10	69 ± 5	0.021	5.02	48.8
EMC3	41 ± 2	286 ± 10	74 ± 5	0.032	6.14	42.9
EMC4	43 ± 2	268 ± 10	73 ± 5	0.024	5.51	42.5

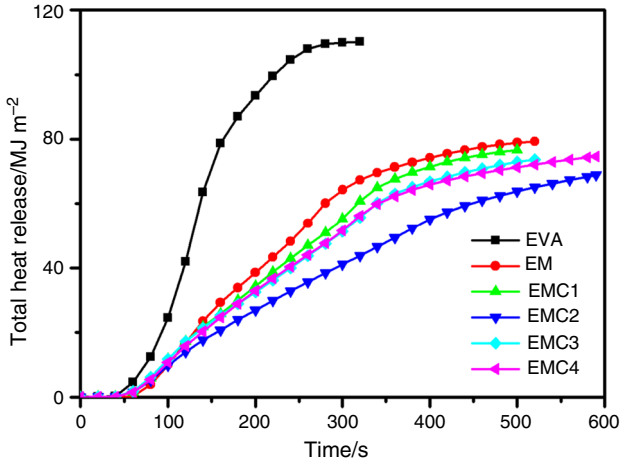

Fig. 3 Total heat release curves of EVA and its composites by cone calorimeter test

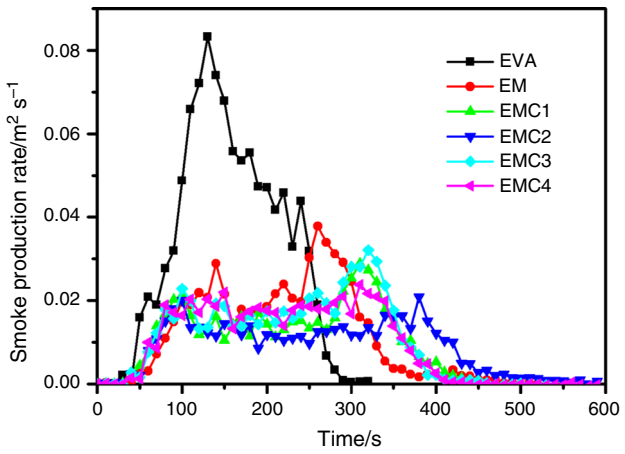

Fig. 4 Smoke production rate curves of EVA and its composites from cone calorimeter test

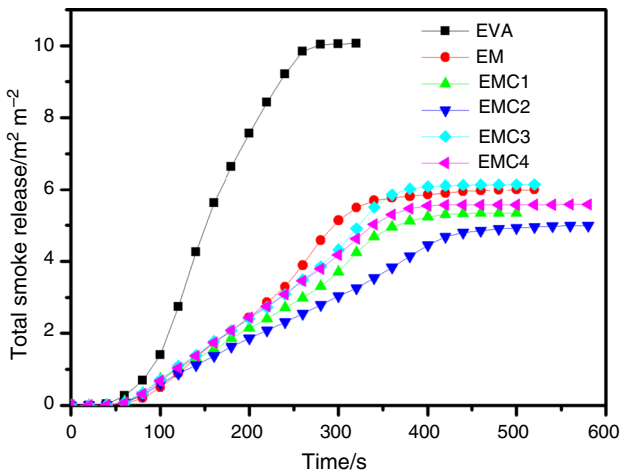

Fig. 5 Total smoke release curves of EVA and its composites from cone calorimeter test

and brucite could produce an obvious smoke suppression in flame-retardant EVA composites.

The structure and morphology of the residual char after cone calorimeter testing were analyzed, which was helpful to clarify the effect of nanofillers during combustion. Therefore, investigating the residual char would provide an insight into the synergistic flame-retardant effects and mechanism of CB in condensed phase. Photographs of the burning residue after cone calorimeter testing are presented in Fig. 6. As shown in Fig. 6a, pure EVA was completely decomposed without any residual char. In Fig. 6b, the EM sample with EVA matrix filled with 55% of brucite presented a thick and hard layer, but it contained large cracks. As it has been demonstrated, magnesium oxide generated and covered the surface of the flame-retardant material, which improved the flame resistance of polymer materials [23]. However, after the CB was added into the EM systems, the sample of EMC illustrated less and thinner residual surface cracks, with compact charred layers on the sample surface. The results indicated that the incorporation of CB and MH could reinforce the thermal stability of the charred layers, which acted as an excellent barrier for mass and thermal transport.

Flame-retardant mechanism

It has been demonstrated that MH can achieve a better flame retardancy due to the endothermic decomposition reaction of MH, which can reduce the EVA surface temperature and free water molecules to dilute the concentrated combustible gas during the combustion. Furthermore, the magnesium oxide builds a protective layer on the composite surface, which cuts off the sources of heat at the point of the combustion and also inhibits the release of flammable gas, thus reducing the flame and smoke effects [22, 23]. Besides, the previous research also demonstrated that carbon black can promote the polymer carbonization to generate a solid-phase flame-retardant mechanism during polymer combustion [16, 37, 38].

To further investigate the flame-retardant mechanism, SEM and EDS were used to investigate the microstructure and elements of char residues and obtain more detailed information about post-thermal degradations. Figure 7 shows the SEM images and EDS of EM and EMC2 from cone calorimeter test. It illustrates (Fig. 7a) that there were lots of holes on the surface of EM charred residue. Therefore, the heat and flammable volatiles could penetrate the char layer into the flame zone during burning. However, Fig. 7b shows the continuous and compact char layer structure on the surface of EMC residue, and there was also almost no flaw or holes on the EMC2 residue. The EDS results showed that the content of carbon on the EMC2

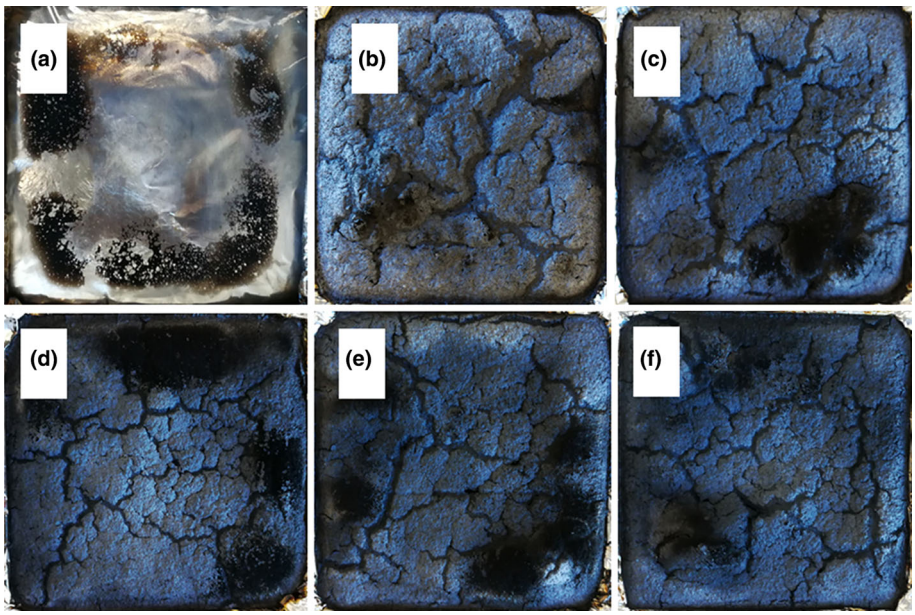

Fig. 6 Digital photographs of the char residues after the cone colorimeter test from **a** pure EVA, **b** EM, **c** EMC1, **d** EMC2, **e** EMC3, **f** EMC4

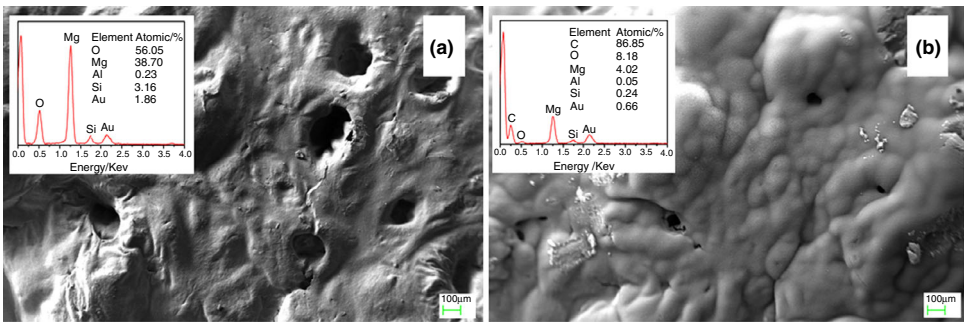

Fig. 7 Microscopic residues of **a** EM and **b** EMC2 at flameout after burning under 50 kW m^{-2}

charred residue surface is more than on EM residue. Apparently, from the above observations, the SEM and EDS results indicated the addition of CB obviously increased the char residue of EVA composites and played synergistic effect on flame-retardant EVA composites with brucite [39].

From the above discussion, we could conclude that the synergistically enhanced flame resistance of EMC composites, due to the carbonization and physical process in the condensed phase. Scheme 1 shows the thermo-decomposition process of flame-retardant EMC composites during burning. The detailed flame-retardant mechanism was proposed as follows. Firstly, when the flame spread onto the surface of the EMC composites, the polymer under the fire passed to a molten state with the decomposition of EVA and brucite, and because of the lower density of CB, it was accumulated on the liquid-phase surface and further promotes the carbonization. Meanwhile, the brucite decomposed into magnesium oxide and water, the water vapor diluted the flammable gases, and the magnesium oxide covered the surface of the composite to isolate the flame. With the burning, the carbon black and magnesium oxide aggregated and formed a barrier layer. Moreover, the cross-linked carbonation between the fillers further improved the stiffness of the condensed phase and restrained the combustion of the composites.

Mechanical properties

According to the research performed, it is demonstrated that CB displayed some positive effects on improving the thermal stability and flame retardancy of EVA composites. The effect of CB on the mechanical properties of EVA was investigated by tensile testing. The detailed data of tensile strength and elongation at break are summarized in

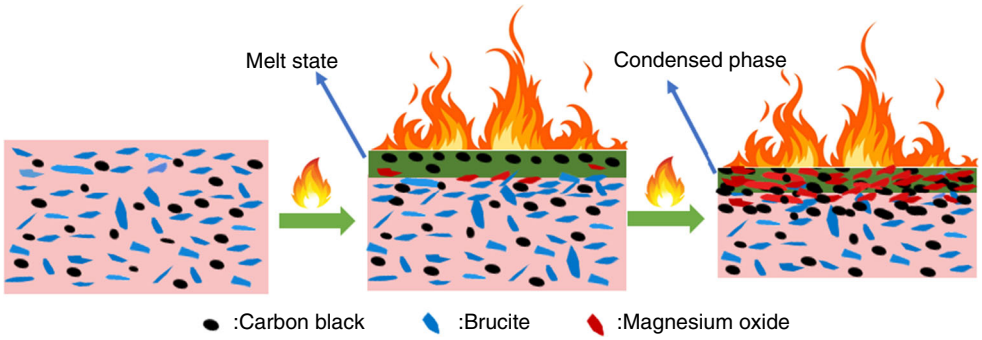

Scheme 1 Schematic illustration of the proceeding combustion of EMC composites

Table 5. The tensile stress and elongation at break of pure EVA were 22.7 MPa and 1297%. It had been observed that the incorporation of brucite and carbon black obviously decreased the mechanical properties of the EM and EMC composites. The tensile strength of EM and EMC composites was between 11 MPa and 12 MPa which had the slight changes; there were also no significant differences in the elongation at break among the composites. It was mainly due to the CB, with nanoparticle size, which can distribute among the bigger particles of brucite [37]. This indicated that small amount of CB particles did not reduce the mechanical properties of EMC composites.

Conclusions

In this paper, the flammability characteristics and thermal degradation behavior of EVA composites with brucite and CB have been compared by melt blending method. TG and DTG results indicated that the addition of CB to the EMC system could improve the thermal stability of the EVA composites. Compared with EVA and EM composites, when 0.5% CB was added into the EM system, the LOI of EMC1 reached a value of 34.8% and passed the V-0 rating in the UL-94 test. With the addition of 1% CB in the EMC system, the LOI of EMC2 further increased, up to 35.3%, and also passed the V-0 rating in the UL-94 test. Combustion behavior obtained from cone calorimeter testing showed that HRR, THR, SPR and TSR for EMC2 were lowest among all the samples. The photographs of residual char showed that adding a moderate quantity of CB would promote the formation of a compact and smooth char structure. The incorporation of CB did not have negative effect on the tensile performance of EVA composites. In summary, a moderate amount of CB imparted EVA/brucite composites an improvement in thermal stability and flame retardancy.

Acknowledgements This work was supported by the Science and Technology of Qinghai Program (No. 2015-HZ-812), the Natural Science Foundation of China (No. U1607104) and the Thousand Talents Plan of Qinghai Province (2017).

References

1. Camino G, Maffezzoli A, De Braglia M, Lazzaro M, Zammarano M. Effect of hydroxides and hydroxycarbonate structure on fire retardant effectiveness and mechanical properties in ethylene-vinyl acetate copolymer. Polym Degrad Stab. 2001;74:457–64.
2. Costache MC, Jiang DD, Wilkie CA. Thermal degradation of ethylene-vinyl acetate coplymer nanocomposites. Polymer. 2005;46:6947–58.
3. Zhou KQ, Tang G, Jiang SH, Gui Z, Hu Y. Combination effect of MoS_2 with aluminum hypophosphite in flame retardant ethylene-vinyl acetate composites. RSC Adv. 2016;6:37672–80.
4. Li Z, Wang J, Expósito DF, Zhang J, Fu C, Shi D, Wang DY. High-performance carrageenan film based on carrageenan intercalated layered double hydroxide with enhanced properties: fire safety, thermal stability and barrier effect. Compos. Commun. 2018;9:1–5.
5. Yu L, Chen L, Dong LP, Li LJ, Wang YZ. Organic-inorganic hybrid flame retardant: preparation, characterization and application in EVA. RSC Adv. 2014;4:17812–21.
6. Kotal M, Bhowmick AK. Polymer nanocomposites from modified clays: recent advances and challenges. Pro Polym Sci. 2015;51:127–87.
7. Wazarkar K, Kathalewar M, Sabnis A. Reactive Modification of Thermoplastic and Thermoset Polymers using Flame Retardants: an Overview. Polym-Plast Technol. 2016;55:71–91.
8. Noh J, Kang I, Choi J, Fatima H, Yoo PJ, Oh KW, Park J. Surface modification of magnesium hydroxide nanoparticles with hexylphosphoric acid to improve thermal stabilities of polyethylene composites. Polym Bull. 2016;73:2855–66.
9. Rothon RN, Hornsby PR. Flame retardant effects of magnesium hydroxide. Polym Degrad Stab. 1996;54:383–5.
10. Pang HC, Wang XS, Zhu XK, Tian P, Ning GL. Nanoengineering of brucite@SiO_2 for enhanced mechanical properties and flame retardant behaviors. Polym Degrad Stab. 2015;120:410–8.
11. Wang XS, Pang HC, Chen WD, Lin Y, Zong LS, Ning GL. Controllable Fabrication of Zinc Borate Hierarchical Nanostructure on Brucite Surface for Enhanced Mechanical Properties and Flame Retardant Behaviors. ACS Appl Mater Inter. 2014;6:7223–35.
12. Liu XW, Wu WH, Qu HQ, Sun JH, Xu JZ. Flame-Retarding and Mechanical Properties of Flexible Polyvinyl Chloride with Surface-Treated Lamellar Magnesium Hydroxide. J Macromol Sci B. 2016;55:115–27.
13. Montezin F, Cuesta JML, Crespy A, Georlette P. Flame retardant and mechanical properties of a copolymer PP/PE containing brominated compounds/antimony trioxide blends and magnesium hydroxide or talc. Fire Mater. 1997;21:245–52.
14. Dittrich B, Wartig KA, Mülhaupt R, Schartel B. Flame-Retardancy Properties of Intumescent Ammonium Poly(Phosphate)

and Mineral Filler Magnesium Hydroxide in Combination with Graphene. Polym. 2014;6:2875.
15. Cabrera Álvarez EN, Ramos-deValle LF, Sánchez-Valdes S, Ramírez-Vargas E, Espinoza-Martinez AB, Rodriguez-Fernandez OS, Beltran-Ramırez FI, Méndez Nonell J. Study of the Effect of a Polymeric Compatibilizing Agent on the Flame Retardancy and Tensile Properties of High Density Polyethylene/Magnesium Hydroxide Compositions. Macromo Symp. 2017;374:1–5.
16. Yang YR, Niu M, Li JJ, Xue BX, Dai JM. Preparation of carbon microspheres coated magnesium hydroxide and its application in polyethylene terephthalate as flame retardant. Polym Degrad Stab. 2016;134:1–9.
17. Zhang T, Liu WS, Wang MX, Liu P, Pan YH, Liu DF. Synergistic effect of an aromatic boronic acid derivative and magnesium hydroxide on the flame retardancy of epoxy resin. Polym Degrad Stab. 2016;130:257–63.
18. Casetta M, Michaux G, Ohl B, Duquesne S, Bourbigot S. Key role of magnesium hydroxide surface treatment in the flame retardancy of glass fiber reinforced polyamide 6. Polym Degrad Stab. 2018;148:95–103.
19. Ye L, Wu QH, Qu BJ. Synergistic effects and mechanism of multiwalled carbon nanotubes with magnesium hydroxide in halogen-free flame retardant EVA/MH/MWNT nanocomposites. Polym Degrad Stab. 2009;94:751–6.
20. Yen YY, Wang HT, Guo WJ. Synergistic flame retardant effect of metal hydroxide and nanoclay in EVA composites. Polym Degrad Stab. 2012;97:863–9.
21. Fu MZ, Qu BJ. Synergistic flame retardant mechanism of fumed silica in ethylene-vinyl acetate/magnesium hydroxide blends. Polym Degrad Stab. 2004;85:633–9.
22. Witkowski A, Stec AA, Richard HT. The influence of metal hydroxide fire retardants and nanoclay on the thermal decomposition of EVA. Polym Degrad Stab. 2012;97:2231–40.
23. Liu L, Hu J, Zhuo JL, Jiao CM, Chen XL, Li SX. Synergistic flame retardant effects between hollow glass microspheres and magnesium hydroxide in ethylene-vinyl acetate composites. Polym Degrad Stab. 2014;104:87–94.
24. Li ZZ, Qu BJ. Flammability characterization and synergistic effects of expandable graphite with magnesium hydroxide in halogen-free flame-retardant EVA blends. Polym Degrad Stab. 2003;81:401–8.
25. Kawamoto M, He P, Ito Y. Green Processing of Carbon Nanomaterials. Adv Mater. 2017;29:1–25.
26. Wang N, Xu G, Wu YH, Zhang J, Hu LD, Luan HH, Fang QH. The influence of expandable graphite on double-layered microcapsules in intumescent flame-retardant natural rubber composites. J Therm Anal and Calorim. 2016;123:1239–51.
27. Zhou KQ, Tang G, Gao R, Jiang SD. In situ growth of 0D silica nanospheres on 2D molybdenum disulfide nanosheets: towards reducing fire hazards of epoxy resin. J Hazard Mater. 2018;344:1078–89.
28. Yang HF, Gong J, Wen X, Xue J, Chen Q, Jiang ZW, Tian NN, Tang T. Effect of carbon black on improving thermal stability, flame retardancy and electrical conductivity of polypropylene/carbon fiber composites. Compos Sci Technol. 2015;113:31–7.
29. Gong J, Niu R, Tian NN, Chen XC, Wen X, Liu J, Sun ZY, Mijowska E, Tang T. Combination of fumed silica with carbon black for simultaneously improving the thermal stability, flame retardancy and mechanical properties of polyethylene. Polymer. 2014;55:2998–3007.
30. Wen X, Wang YJ, Gong J, Liu J, Tian NN, Wang HH, Jiang ZW, Qiu J, Tang T. Thermal and flammability properties of polypropylene/carbon black nanocomposites. Polym Degrad Stab. 2012;97:793–801.
31. Dittrich B, Wartig KA, Hofmann D, Mülhaupt R, Schartel B. Flame retardancy through carbon nanomaterials: carbon black, multiwall nanotubes, expanded graphite, multi-layer graphene and graphene in polypropylene. Polym Degrad Stab. 2013;98:1495–505.
32. Guan FL, Gui CX, Zhang HB, Jiang ZG, Jiang Y, Yu ZZ. Enhanced thermal conductivity and satisfactory flame retardancy of epoxy/alumina composites by combination with graphene nanoplatelets and magnesium hydroxide. Compos Part B-Eng. 2016;98:134–40.
33. Etika KC, Liu L, Hess LA, Grunlan JC. The influence of synergistic stabilization of carbon black and clay on the electrical and mechanical properties of epoxy composites. Carbon. 2009;47:3128–36.
34. Presti C, Ferry L, Alauzun JG, Dumazert L, Gallard B, Quantin JC, Lopez Cuesta JM, Mutin PH. Functionalized nanodiamond as potential synergist in flame-retardant ethylene vinyl acetate. Diam Relat Mater. 2017;76:141–9.
35. Li Z, Expósito DF, González AJ, Wang DY. Insightful investigation of smoke suppression behavior and mechanism of polystyrene with ferrocene: an important role of intermediate smoke. Fire Mater. 2018;42:286–95.
36. Jian RK, Wang P, Duan W, Wang JS, Zheng XL, Weng JB. Synthesis of a Novel P/N/S-Containing Flame Retardant and Its Application in Epoxy Resin: thermal Property, Flame Retardance, and Pyrolysis Behavior. Ind Eeg Chem Res. 2016;55:11520–7.
37. Chen Q, Wen X, Chen H, Qi YL, Gong J, Yang HF, Li YH, Tang T. Study of the effect of nanosized carbon black on flammability and mechanical properties of poly(butylene succinate). Polym for Advan Technol. 2015;26:128–35.
38. Wang X, Kalali EN, Wan JT, Wang DY. Carbon-family materials for flame retardant polymeric materials. Prog Polym Sci. 2017;69:22–46.
39. Ye L, Miao YY, Yan H, Li Z, Zhou YL, Liu JX, Liu H. The synergistic effects of boroxo siloxanes with magnesium hydroxide in halogen-free flame retardant EVA/MH blends. Polym Degrad Stab. 2013;9:868–74.